

C02 Gasification Behavior of Various Biomass Chars -Effect of Mineral Matters in Biomass Chars-

著者	Ikenaga Naoki, Nakajima Hiroshi, Oda Hirokazu, Suzuki Toshimitsu
journal or publication title	Science and Technology reports of Kansai University = 関西大学理工学研究報告
volume	51
page range	61-74
year	2009-03-20
URL	http://hdl.handle.net/10112/921

CO₂ Gasification Behavior of Various Biomass Chars — Effect of Mineral Matters in Biomass Chars —

Na-oki IKENAGA*, Hiroshi NAKAJIMA, Hirokazu ODA, Toshimitsu SUZUKI

(Received October 4, 2008)

Abstract

In order to develop the effective utilization of biomass, the gasification behavior of various chars prepared from biomass (mostly garden trees) was studied. The gasification rate was affected by the content of indigenous mineral matter such as calcium and potassium. The gasification behavior of chars were classified into 3 groups, as follows: (i) the gasification rate reached a maximum in the higher conversion region, (ii) the gasification rate profile showed two peak values, (iii) the gasification rate profile fitted the random pore model.

An increase in the gasification rate in a higher char conversion region contributed to the promotion effect of the potassium catalyst. The number of active centers in the char was obtained by the O₂ uptake at an ambient temperature using pulse technique. The number of active sites was increased by mineral matter and the disintegration of the char structure.

Keywords: CO₂; gasification; biomass; mineral matter

1. Introduction

In the 3rd Session of the Conference of the Parties to the United Nations Framework Convention on Climate Change (COP3), developed countries were obligated to decrease their emission of greenhouse gases. To achieve the treaty's goal, countries have to develop their use of non-fossil fuels to replace fossil fuels.

Biomass is one of such alternatives with which to reduce CO₂ emission. Biomass is composed of similar organic sources to coal, but it is carbon neutral source. The CO₂ concentration on the land surface is considered not to vary in spite of releasing CO₂ by combustion of biomass, since CO₂ is absorbed by photosynthesis when new biomass grows. Clean development mechanism (CDM) projects, as defined by the Kyoto Protocol, could be achieved by getting more than 40 % of energy sources from biomass¹⁾. The CDM projects related to biomass are construction of power generation plants using biomass, the use of bio-gas and the use of bio-diesel fuels. An integrated system at a gasification power plant is effective to reduce CO₂ emissions. This technology is of importance.

*Corresponding author: Department of Chemical, Energy & Environmental Engineering, Kansai University.

E-mail: ikenaga@ipcku.kansai-u.ac.jp

In the gasifier, a gasification agent such as O₂, air, steam, and CO₂ are used, and the reaction of CO₂ and H₂O with biomass char is the rate-determining step. Therefore, analysis of the reaction of char with CO₂ and H₂O is an important factor in designing a gasification plant.

In terms of carbon gasification, Walker et al. proposed the idea of active surface area (C_f), the number of active sites, which has a good correlation with the reaction rate of carbon^{2, 3}. The mechanism of non-catalytic carbon gasification processes are understood as:



where C_f and C(O) denote a free carbon active site and an occupied active site. Desorption of C(O) to give CO regenerates a free C_f active site.

A large number of studies on coal char gasification have been carried out. Takeda et al. reported that the gasification rate is affected by the rank of coal, carbonization conditions, and the graphite structure developed during gasification at high temperature⁴. Furthermore, use of catalyst for coal gasification is proposed in order to decrease gasification temperature without changing gasification rate. Transition metals (Ni, Fe)⁵⁻¹⁰, alkali metals (Li, Na, K, Rb)¹¹⁻¹⁵, and alkaline earth metals (Ca, Mg, Sr, Ba)^{13, 16, 17} showed high activities in the coal char gasification. In addition, mineral matter contained in coal affects the reactivity of coal. Hashimoto et al. investigated the steam gasification of 18 different raw and demineralized coals, and found that the gasification rate of low rank coals (C<80%) was decreased by demineralization, and that the gasification rate of high rank coal did not change. Rather, the rate of some coals increased¹⁸.

Many attempts have been made to develop a kinetic model for CO₂ gasification behavior of coal chars, i.e. the grain model¹⁹, the percolation model²⁰, or the random pore model (RPM)²¹. In biomass gasification, however, the presumptions based on the original model derivation do not match experimental value, especially not with catalyzed char gasification²². Although the deviation from gasification behavior occurred in a high conversion region, Standish et al. pointed out that it might emerge from a sudden disintegration of porous structure during gasification²³. Hamilton et al. proposed the reason for the reaction rate being at a maximum at around conversion of 0.7 was surface saturation of biomass char by the alkali catalyst²⁴. This suggestion, however, is not consistent with other literature²⁵ on saturation effects in alkali-catalyzed gasification of biomass chars. It is claimed that the initial reaction rate of chars impregnated with alkali carbonates increases uniformly with the metal-to-carbon atom ratio (M/C), up to a saturation level, typically, of M/C = 0.1. Although initial atomic M/C ratio of chars impregnated with alkali metal is ca. 0.007, the saturation effects at M/C = 0.1 may not be encountered below 93 % of the carbon consumed by the gasification reaction. Struis et al. have insisted that anomalous reaction rate behavior with alkali-catalyzed char merely depicts a superposition of changes of structure (micropore domain) and catalytic effects²².

All the mineral matters in biomass are composed in part of tissue. The char from plants is considered to be more homogeneous than that of coal char. In addition, demineralization of biomass can easily be carried out simply by immersing in dilute HCl.

From this standpoint, the study of CO₂ gasification of various biomass chars looks

promising in terms, not only of effective utilization of biomass, but also of gasification of carbon sources, and specifically catalytic gasification.

In this paper, we describe the CO₂ gasification behavior of various wood chars, and examine them to understand the effect of the mineral matters contained in biomass on the gasification rate.

2. Experimental

2.1 Feedstock

Japanese cedar wood, fig tree, umemodoki (*Ilex serrata*), Japanese oak, mukuge (*Hibiscus syriacus*), eucalyptus, cherry tree, satsuki (*Rhododendron indicum*), chopstick (*Betula platyphylla*), nandina, and pine were used as woody biomass samples; bean curd, coffee bean residue, and tea leaves as food wastes; rice straw as herbaceous biomass; and chlorella, rittorale, and spirulina as microalgae biomass. Australian Yallourn coal and Japanese Taiheiyo coal were used to compare with the biomass.

NaCO₃, K₂CO₃, Ca(OH)₂, (CHCOO)₂Ca·H₂O, Mg(NO₃)₂·6H₂O, and Fe(NO₃)₃·9H₂O were reagent grade chemicals from Wako Pure Chemical Industries Ltd.

2.2 Acid treatment

5 g of ground biomass (< 1 mm) was demineralized using 100 mL of 1 M hydrochloric acid for 12 h under supersonic radiation. Then the samples were washed with pure water until Cl free and dried in vacuo at 70 °C for 24 h.

2.3 Impregnation of catalysts

A solution of NaCO₃, K₂CO₃, Ca(OH)₂, (CHCOO)₂Ca·H₂O, Mg(NO₃)₂·6H₂O, or Fe(NO₃)₃·9H₂O was mixed with a 0.5 g of HCl treated biomass or a 0.1 g of char. The slurry was stirred for 24 h, and then the excess water was removed at 70 °C under reduced pressure using a rotary evaporator.

2.4 Char preparation

Untreated or HCl-treated samples were devolatilized at 1000 °C at a heating rate of 10 °C/min for 2 h under nitrogen atmosphere. The obtained chars were pulverized to pass through a 100 mesh screen.

2.5 Characterization

Alkali metals, alkaline earth metals, and iron contents were obtained by inductively coupled plasma atomic emission spectrometry (Shimadzu ICP-1000 III) and atomic absorption spectrometry (Shimadzu AA-6800) from the recovered HCl solution after treating biomass samples. Silicon and aluminum contents were measured by a sequential X-ray fluorescence spectrometer (Shimadzu SXF-1200BF) from biomass ash. Anhydrous lithium tetraborate (type II) and ash were set in a sample holder made from polyvinyl chloride, which was pressurized at 8 t for 10 min. Monochromated X-rays were irradiated from a RhKa target (tube voltage: 40 kV, tube current: 70 mA).

The surface areas of the chars were measured by the BET method using an automatic gas

adsorption apparatus (Yuasa Ionics Co., Autosorb-1), applying adsorption isotherms of nitrogen at $-196\text{ }^{\circ}\text{C}$. Surface areas of selected biomass chars were measured by the Dubinin-Astakhov method applying adsorption isotherms of carbon dioxide at $0\text{ }^{\circ}\text{C}$.

The true density measurement was performed by vapor replacement method with He using a Micromeritics gas pycnometer (Shimadzu Accupyc 1300).

The structure of chars was analyzed by powder X-ray diffraction method using an X-ray diffractometer (Shimadzu XRD-6000) with monochromatized $\text{CuK}\alpha$ radiation (tube voltage: 40 kV, tube current: 30 mA).

2.6 Gasification

The gasification of char was conducted using a thermogravimetric analyzer (Shimadzu TGA-50). A 10 mg of char was placed on the platinum pan. Heating was programmed at a heating rate of $20\text{ }^{\circ}\text{C}/\text{min}$ from room temperature to $800\text{--}1000\text{ }^{\circ}\text{C}$ under N_2 atmosphere. After 1 h of heating, N_2 flow was switched to CO_2 (30 mL/min) and weight loss was monitored. Remaining carbon was burned off after the gasification by air. Conversion X and the gasification rate R during gasification were calculated as follows;

$$X = (M_0 - M_t) / (M_0 - M_{\text{ash}}) \quad (4)$$

$$R = 1 / (1 - X) (dX / dt) \quad (5)$$

where M_0 , M , M_{ash} are initial weight, weight at t , and weight of ash, respectively.

2.7 Evaluation of gasification rate

An attempt to fit the gasification rate to the random pore model proposed by Bhatia and Pulmutter was carried out to describe gasification behavior²⁰. The kinetic model assumed that the reaction proceeds randomly on the surface of pores in the solid char. The degree of pore erosion in the reaction progress is represented as

$$S = S_0(1 - X)(1 - \psi n(1 - X))^{1/2} \quad (6)$$

$$\psi = 4\pi_0(1 - \rho_t) / S_0^2 \quad (7)$$

in which ψ , L_0 , ρ_t , S_0 and S denotes a dimensionless parameter of porous structure, length per unit volume, porosity, initial surface area and surface area at t , respectively. Assuming that the reaction occurs on the solid surface and the pore is cylinder hollow, eq. (6) and (7) rewrites

$$dX / dt = k_p(1 - X)(1 - \psi n(1 - X))^{1/2} \quad (8)$$

$$\psi = 1 / \rho_t V_0 \quad (9)$$

The reaction rate constant k_p is obtained by least square fitting of the eq. (8) to the experimental gasification behavior. The ψ is represented by using the true density ρ_t and volume per unit gram V_0 .

2.8 Oxygen uptake measurement of cedar wood char and cedar wood HCl char

O₂ pulsed adsorption experiments were carried out to determine the carbon active sites. 30 mg of char was introduced into a reactor connected to a TCD detector. Pretreatment was carried out in a He stream at 650 °C for 1 h (He flow rate: 20 mL/min). Then the sample was cooled down to 200 °C and O₂ (1 mL/pulse) was pulsed over the char until the detection responses became constant.

3. Results and Discussion

3.1 Physical properties and metal contents

Table 1 summarizes indigenous metal constituents, water, and ash contents in raw biomass, and char yield from various biomass sources. Water content was calculated by a weight loss from as received and crushed sample after drying at 107 °C for 1 h in an oven. The amount of ash in the biomass was obtained by burning biomass chars in air flow after gasification experiments at 900 °C.

Metal contents in various types of biomass sources vary greatly. In woody biomass, potassium and calcium are the major catalytically active elements in the gasification, and small amounts of silicon and aluminum are contained. On the contrary, herbaceous biomass and coal contain large quantities of silicon and aluminum. The microalgae biomass contains a great amount of ash.

Char yields of biomass at 1000 °C were 16-39 wt% (d.b.), and these were smaller as compared to those of coals (50-57 wt% (d.b.)). On the other hand, char yields of demineralized biomass were slightly larger than those of raw biomass. The conversion of tar during the pyrolysis is assumed to decrease as a result of mineral matters after demineralization treatment.

Surface areas of biomass chars obtained from nitrogen adsorption at 77 K were in the range of 66-342 m²/g. However, surface areas calculated from carbon dioxide adsorption at 298 K are higher than those observed for nitrogen. The surface areas calculated from carbon dioxide adsorption of cedar wood char, cedar wood treated HCl char (cedar wood HCl char) and fig tree char were nearly ten times as large as those calculated from nitrogen adsorption (879-1144 m²/g). It is said that pore diameter of char is mostly the same size as the gas molecule and therefore nitrogen takes a long time to diffuse into the pores²⁶⁾. Here, the surface areas calculated from nitrogen at 77 K were compared and the pore volume V₀ obtained from carbon dioxide adsorption at 298 K was employed for kinetic model parameters.

According to XRD measurements of various biomass types and coal chars. Peaks ascribed to graphite (002) and (100) structure were observed at $2\theta = 26.5^\circ$ and 43.5° , but all the samples showed only broad peaks of amorphous structure. Therefore, it is obvious that the graphite structure did not grow in chars prepared here.

3.2 Gasification of various biomass chars

Gasification behavior of biomass chars and coal chars is shown in Figs. 1-4. Gasification behavior of chars was classified into 3 groups, as follows: (i) the gasification rate reached a maximum in the higher conversion region ($X =$ around 0.7), e.g. fig tree, oak, cedar wood, satsuki, nandina, coffee residue, tea residue, dry bean curd, and pine; (ii) the gasification rate

Table 1. Physical properties and metal constituents of various biomass sources

Sample	Source	Treatment	Raw biomass									Charcoal		
			Metal content (mmol/100 g-biomass d.b.)							Ash (wt% d.b.)	Water (wt%)	Char yield (wt% d.b.)	S.A. ¹⁾ (m ² /g)	Gasification time ²⁾ (min)
			Na	K	Mg	Ca	Fe	Si	Al					
1	fig tree	-	0.22	37.47	6.42	16.93	0.02	0.07	5.35	3.5	9.6	28.2	74	19
2	umemodoki		0.04	8.34	6.42	16.78	0.02	0.17	4.20	2.5	8.3	22.8	184	27
3	oak		0.43	13.27	1.69	13.73	0.39	0.09	5.30	2.2	7.4	24.7	92	27
4	mukuge		0.39	12.27	4.57	23.58	0.05	0.26	1.47	2.9	8.3	26.6	66	29
5	eucalyptus		1.80	4.75	0.50	2.52	0.05	0.23	2.37	0.6	9.8	23.6	233	33
6	sawdust		0.80	1.76	0.70	5.35	0.07	0.68	4.66	0.8	5.8	21.4	71	38
7	cherry tree		0.17	2.23	0.66	9.68	0.04	0.09	1.00	1.9	8.9	19.5	293	40
8	cedar wood		0.17	5.37	0.33	1.23	0.04	0.47	2.04	0.5	9.6	25.1	155	51
9	satsuki		0.13	5.47	2.02	3.15	0.07	0.11	2.20	1.3	24.7	31.2	277	57
10	chopstick		0.09	2.12	0.82	1.28	0.02	0.22	1.29	0.4	7.4	16.8	342	63
11	nandina		1.17	6.62	1.40	5.83	0.04	0.61	6.09	1.1	8.4	24.2	98	81
12	pine		2.02	1.10	0.26	0.57	0.02	0.11	3.72	0.4	9.1	22.8	182	113
13	coffee residue	-	0.52	12.14	4.63	2.57	0.09	0.28	2.64	4.7	4.9	20.8	30	40
14	tea residue		0.66	12.16	5.53	9.04	0.26	6.51	40.63	13.6	3.3	25.8	35	76
15	dry bean curd		5.00	37.10	6.02	6.64	0.09	0.55	6.03	2.8	0.6	21.2	14	46
16	dry chlorella	-	16.65	48.54	11.90	2.64	1.17	0.81	10.20	4.3	6.2	20.3	56	315
17	dry rittorale		15.22	99.67	13.01	2.77	0.07	3.17	38.82	16.4	9.9	22.6	291	54
18	dry spirulina		14.31	49.51	13.68	3.68	0.08	1.15	9.13	3.8	8.5	20.6	41	165
19	rice straw	-	0.83	77.16	4.53	5.95	0.14	30.44	23.85	15.7	16.4	38.5	77	91
20	Yallourn coal	-	2.78	0.03	6.67	3.50	6.46	0.28	12.45	1.8	5.6	50.5	308	41
21	Taiheiyo coal		2.83	0.08	2.84	17.70	0.30	26.22	115.24	11.2	5.9	57.0	48	266
22	fig tree									0.4		25.9		661
23	eucalyptus									0.4		22.9	-	751
24	cherry tree									0.2		21.1		603
25	cedar wood	HCl	-	-	-	-	-	-	-	0.3	-	23.6	236	1071
26	chopstick									0.3		17.7		594
27	nandina									0.4		25.6	-	594
28	Yallourn coal									0.8		51.8		413

1) S.A. = Surface Area (N₂ BET)

2) Experimental gasification time measured by thermogravimetric analyzer

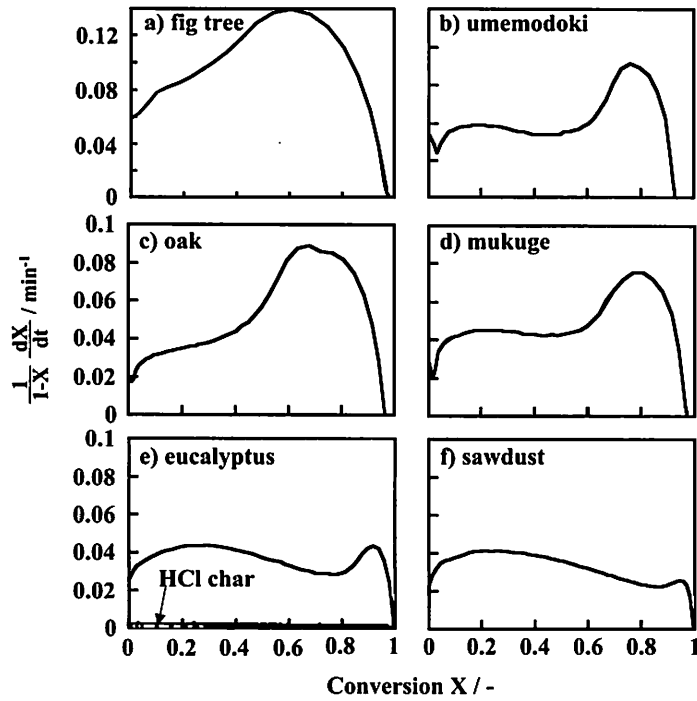


Fig. 1 Gasification behavior of various biomass chars
 Conditions; heating rate: 20°C/min, temperature: 900°C,
 gasification agent: CO₂ 30mL/min, amount: 10mg

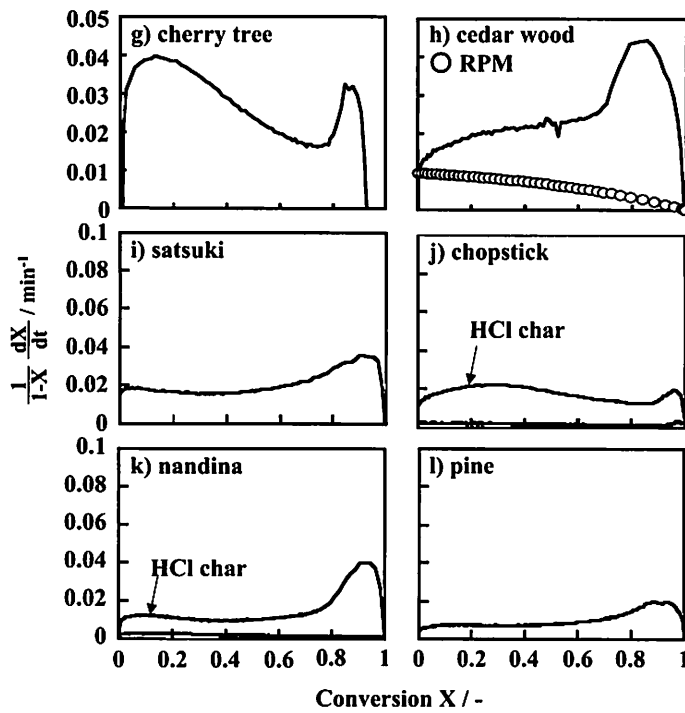


Fig. 2 Gasification behavior of various biomass chars (cont. from Fig. 1)
 Conditions; heating rate: 20°C/min, temperature: 900°C,
 gasification agent: CO₂ 30mL/min, amount: 10mg

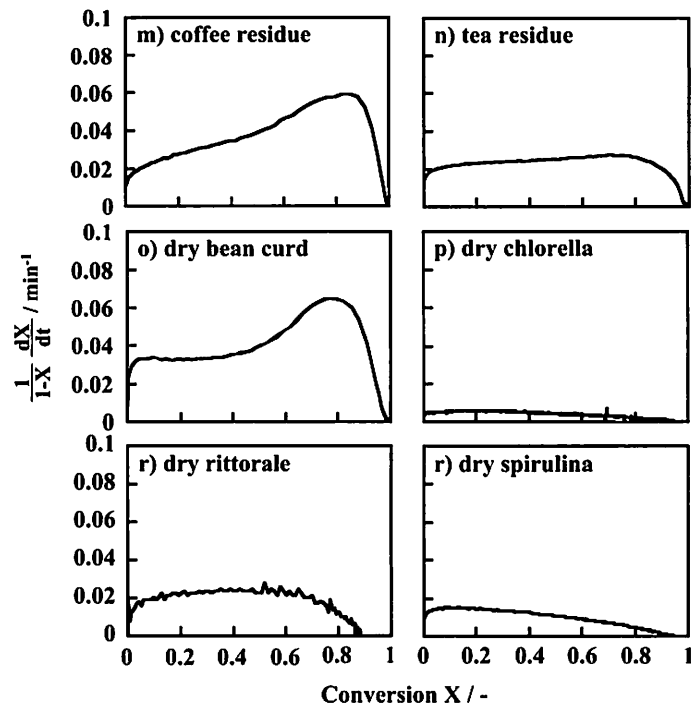


Fig. 3 Gasification behavior of various biomass chars (cont. from Fig. 1)
 Conditions; heating rate: 20°C/min, temperature: 900°C,
 gasification agent: CO₂ 30mL/min, amount: 10mg

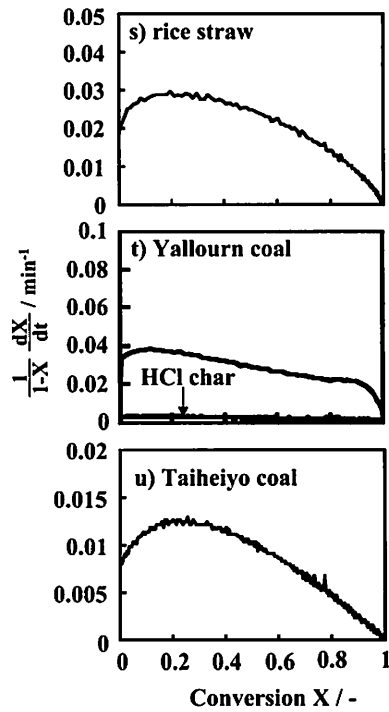


Fig. 4 Gasification behavior of various biomass chars (cont. from Fig. 1)
 Conditions; heating rate: 20°C/min, temperature: 900°C,
 gasification agent: CO₂ 30mL/min, amount: 10mg

profile showed two peaks, e.g. umemodoki, mukuge, eucalyptus, sawdust, cherry tree, and chopstick; (iii) gasification rates did not show sharp increases, e.g. dry chrorella, dry rittorale, dry spirulina, rice straw, Yallourn, and Taiheiyo coal.

As a representative of group (i), cedar wood (Sample 8, Fig. 1) is a typical woody biomass, and the gasification rate of the char increased at the initial stage and remained constant to char conversion of 70% ($X = 0.7$). Gasification rate increased rapidly at above the conversion X of 0.7 and a maximum rate was obtained at X of around 0.8. Well-known kinetic models like the random pore model proposed by Bhatia and Perlmutter fail to describe the pronounced acceleration in the reaction rates. Fig tree char (group (i)) showed the largest gasification rate among all the samples (Sample 1, Fig. 1). Since fig tree contains a large amount of potassium and calcium (especially potassium), indigenous metals seemed to catalyze the gasification of the char. Containing a relatively large amount of potassium in the char is characteristic of group (i).

As a representative of group (ii), umemodoki and mukuge (Samples 2 and 4, Fig. 1) contained a large amount of both potassium and calcium. The gasification rate profiles of these chars exhibited two peaks at $X =$ around 0.2 and 0.8, and this profile did not fit the random pore model.

The gasification behavior of rice straw containing a large amount of potassium (group (iii), Sample 19, Fig. 4) exhibited similar behavior to that of Taiheiyo coal (Sample 21, Fig. 4). However, rice straw contains significant amounts of silica, and as a result during the pyrolysis of the biomass, silica may deactivate potassium by forming catalytically inactive potassium silicate, leading to reduced char gasification rates²⁷⁾. The microalgae biomass chars contained a large amount of metals, but the chars showed low reactivity (Fig. 3). Alkali and alkaline earth metals exist in the form of chloride, so that the metals did not exhibit catalytic activity during gasification.

The ash constituents of biomass seemed to effect gasification rate much more than the surface areas of chars.

3.3 Gasification of acid-treated biomass chars

Fig. 5 shows the gasification behavior of demineralized cedar wood char (Sample 25). Compared to Fig. 2, it is evident that the absence of indigenous mineral matters in cedar wood HCl char led to a markedly decreased gasification rate as compared with that of the original one. Especially, a steep rise in the gasification rate of cedar wood char gasification at X near 0.7 disappeared. Thus, the random pore model fitted well with experimental results, and predicted gasification time of 1050 min at X of 0.99 was in good agreement with the experimental gasification time of 1071 min. The indigenous mineral matters such as alkali and alkaline earth metals in the biomass were easily removed from the biomass, but the silica and alumina contained in the biomass were difficult to remove²⁸⁾. Therefore, it is apparent that the decrease in the gasification rate may be attributed to removal of alkali and alkaline earth metals, whereas mineral matter greatly affected the biomass gasification.

3.4 Re-impregnation of alkali and alkaline earth metals to demineralized cedar wood

In order to understand the catalytic effects of the mineral matters in detail, addition of sodium, magnesium, iron, potassium, and calcium to demineralized cedar wood was examined. Fig. 6 summarizes gasification behavior of demineralized cedar wood char after impregnating

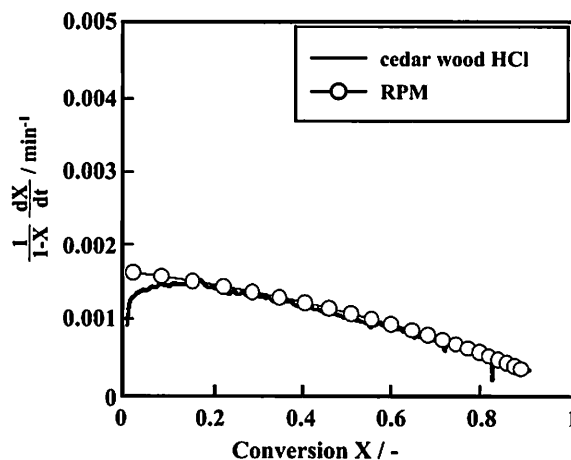


Fig. 5 Gasification behavior of HCl-treated cedar wood char and fitting random pore model
 Conditions; heating rate: 20°C/min, temperature: 900°C,
 gasification agent: CO₂ 30mL/min, amount: 10mg

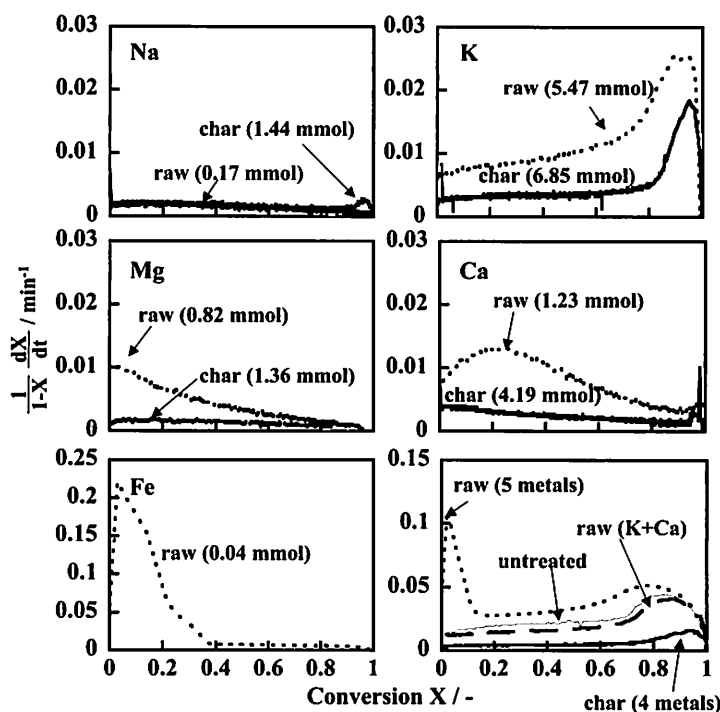


Fig. 6 Catalysis of various mineral matter on HCl-treated cedar wood
 Conditions; heating rate: 20°C/min, temperature: 900°C,
 gasification agent: CO₂ 30mL/min, amount: 10mg

different amounts of metal salts. The term “raw” in Fig. 6 indicates the gasification behavior of the char prepared by impregnating on demineralized raw biomass before carbonization, and “char” indicates behavior of the char impregnated after carbonization of demineralized biomass. The char impregnated after carbonization showed lower reactivity than the char impregnated before carbonization.

In the gasification of sodium-impregnated char, no catalytic effect of sodium was observed.

Magnesium and iron increased the gasification rate at X to below 0.2, and the gasification behavior of magnesium and iron-impregnated char did not agree with that of the char prepared from the untreated cedar wood. When potassium and calcium were impregnated, the gasification rate was enhanced at X to about 0.9 and 0.3, respectively. Both potassium and calcium were then impregnated in the demineralized cedar wood. The impregnation of these metals reproduced the gasification behavior of the untreated cedar wood char.

3.5 Effects of loading level of calcium or potassium on HCl-treated cedar wood

The effects of the loading level of calcium or potassium catalyst were examined. The initial gasification rate increased with increasing loading level of calcium from 0.62 to 2.46 mmol/100g-biomass (Fig. 7). However, gasification rate decreased with an increase in the char

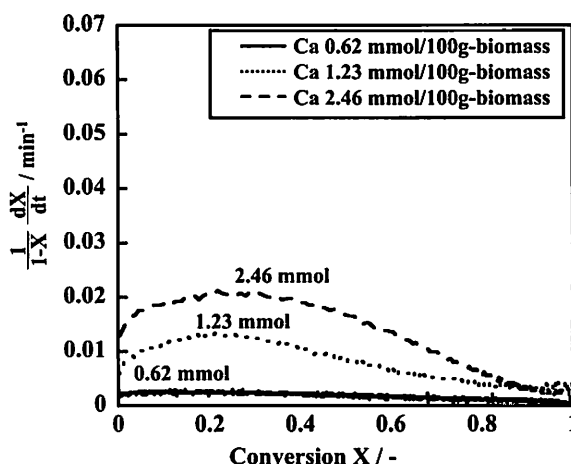


Fig. 7 Effect of Ca loading level on HCl-treated cedar wood char
 Conditions; heating rate: 20°C/min, temperature: 900°C,
 gasification agent: CO₂ 30mL/min, amount: 10mg

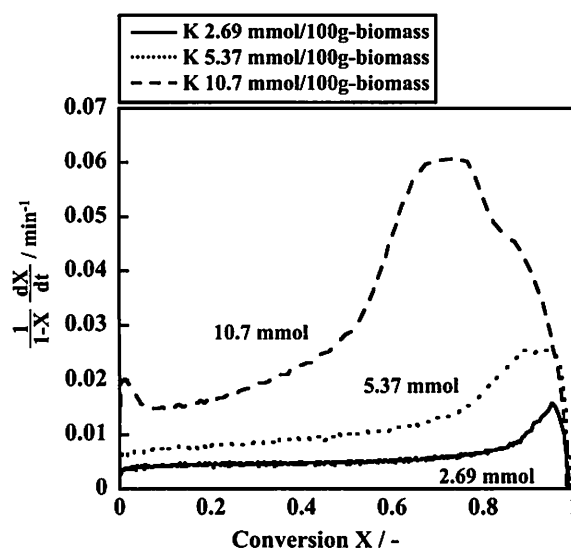


Fig. 8 Effect of K loading level on HCl-treated cedar wood char
 Conditions; heating rate: 20°C/min, temperature: 900°C,
 gasification agent: CO₂ 30mL/min, amount: 10mg

conversion. Calcium exists in the form of calcium oxide in the char, and this oxide sintered gradually during the gasification as evidenced by XRD measurement after gasification. The calcium deactivated mostly around X of 0.8, and the gasification rate decreased regardless of loading level. On the other hand, in the coal gasification with calcium oxide, the gasification rate increased at X to above 0.8²⁸⁾. The catalytic effect of calcium oxide on the gasification of biomass is different from that on the coal gasification.

On the contrary, the potassium catalyst promoted the gasification rate gradually (Fig. 8), a steep rise at the higher conversion ($X > 0.7$) was observed as well as in the gasification behavior of untreated cedar wood char. The maximum gasification rate increased in proportion to the loading level of potassium. It is obvious that the gasification of biomass char depends on the catalytic effects of potassium and calcium.

3.6 Oxygen uptake measurement of cedar wood char and cedar wood HCl char

The mechanism of alkali metal catalysis in the CO_2 gasification of carbon is complex, but has been proposed as the following simplified oxygen-transfer processes²⁹⁾:



where C_f is a free carbon active site. It is thought that the free carbon active site exists on the edge of graphene sheets.

Potassium catalyst disperses well on carbon up to atomic level, since it is in liquid or vapor state at a gasification temperature^{30, 31)}. Thus contact between metal and carbon is possible, irrespective of carbon conversion. Since the metal-to-carbon ratio increases constantly with progress in the gasification, the gasification rate should continue to increase until the end of gasification. However, the gasification rate reached a maximum at X of around 0.7 in the gasification of the cedar wood char. In order to examine this phenomenon in detail, the untreated cedar wood char or the HCl-treated char at conversion levels of 0.2, 0.6, and 0.7 was prepared in large amounts and the oxygen pulsed adsorption technique was applied to measure the amount of O_2 chemisorption. The amount of O_2 uptake should reflect the amount of free carbon active sites in the char. Table 2 shows O_2 uptake of the chars at various conversion levels. O_2 uptake of the untreated char was much larger than that of the HCl-

Table 2. Comparison of surface area and O_2 uptake

Sample	X	S.A.	O_2 uptake
	(-)	(m^2/g)	($\mu\text{mol}/\text{g-char}$)
cedar wood	0	155	116
	0.24	778	221
	0.62	756	325
	0.73	1016	419
cedar wood HCl	0	236	23
	0.24	1001	31
	0.64	2761	25

treated char.

O₂ uptake of the HCl-treated cedar wood char did not change during gasification, although the amount of free carbon active sites should increase with an increase in the surface area of the char. In other words, the number of free carbon active sites on the surface of the char did not increase even if the surface area of the char increased. This is because the absolute amount of char decreased with increased conversion. Thus, the O₂ uptake would decrease with any further progress of the gasification. This fact is consistent with the gasification behavior of the HCl-treated char, indicating a relatively constant gasification rate (Fig. 5).

On the other hand, O₂ uptake of the untreated cedar wood char increased with an increase in the surface area as the gasification progressed. In the same manner as with the HCl-treated cedar wood char, the number of free carbon active sites may not increase. However, the gasification rate was promoted to X of around 0.7 by increasing catalyst (mainly potassium)-to-carbon ratio. The gasification rate decreases rapidly at X of above 0.7, because the amount of remaining char decreases (Fig. 2). It is predicted that the steep rise until X of around 0.7 is caused by the potassium catalyst, which can easily move to the active free carbon sites made available by the fragmentation of carbon structure. The observation of the disintegration of char structure, as reported by Standish et al.²²⁾, supports our proposed mechanism.

4. Conclusion

Gasification behavior of various biomass chars was investigated. The gasification rate was affected by indigenous mineral matter content of calcium and potassium. A steep rise in the higher conversion region was assumed to be caused by potassium catalyst moving to the active free carbon sites made available by the fragmentation of carbon structure. The results of O₂ uptake by pulse techniques reflect the gasification rate, and the increase in free carbon active sites with an increase in the conversion.

Acknowledgements

This research was financially supported in part by the Kansai University Grant-in-Aid for progress in research in a graduate course, 2006.

References

- 1) Yoshitaka M., *J. Jpn. Inst. Energy*, 84, 815 (2005)
- 2) Laine N.R., Vastola F.J., Walker Jr. P.L., *J. Phys. Chem.*, 67, 2030 (1963)
- 3) Radovic L.R., Walker Jr. P.L., Jenkins R.G., *Fuel*, 62, 849 (1983)
- 4) Takeda S., Kitano K., Kubota J., Kawabata J., *J. Fuel. Soc. Jpn.*, 64, 409 (1985)
- 5) Tomita A., Oikawa Y., Kanai T., Tamai Y., *Fuel*, 58, 614 (1979)
- 6) Haynes W.P., Gasior S.J., Forney A.J., *Adv. Chem. Ser.*, 131, 179 (1974)
- 7) McKee D.W., *Carbon*, 12, 453 (1974)
- 8) Baker R.T.K., Chludzinski J.J.Jr., Sherwoo R.D., *Carbon*, 23, 245 (1985)
- 9) Inui T., Otowa T., Okazumi F., *Carbon*, 23, 195 (1985)
- 10) Tanaka S., U-emura T., Ishizaki K., Nagayoshi K., Ikenaga N., Ohme H., Suzuki T., *Energy Fuels*, 9,

45 (1995)

- 11) Kayembe N., Pulsifer A.H., *Fuel*, 55, 211 (1976)
- 12) Veraa M.J., Bell A.T., *Fuel*, 57, 1941 (1978)
- 13) Huttinger K.J., Minges R., *Fuel*, 64, 486 (1985)
- 14) Takarada T., Nabatame T., Ohtsuka Y., Tomita A., *Energy Fuels*, 1, 308 (1987)
- 15) Takarada T., Nabatame T., Ohtsuka Y., Tomita A., *Ind. Eng. Chem. Res.*, 28, 505 (1989)
- 16) McKee D.W., *Fuel*, 59, 308 (1980)
- 17) Yamada T., Honma T., Suzuki T., *J. Fuel. Soc. Jpn.*, 62, 974 (1983)
- 18) Hashimoto K., Miura K., Xu J.J., *J. Fuel. Soc. Jpn.*, 66, 418 (1987)
- 19) Szekely J., Evans J.W., *Chem. Eng. Sci.*, 26, 1901 (1971)
- 20) Sahimi M., Gavalas G.R., Tsotsis T.T., *Chem. Eng. Sci.*, 45, 1443 (1990)
- 21) Bhatia S.K., Perlmutter D.D., *AIChE J.*, 26, 379 (1980)
- 22) Struis R.P.W.J., Scala C.V., Stucki S., Prins R., *Chem. Eng. Sci.*, 57, 3593 (2002)
- 23) Standish N., Tanjung A.F.A., *Fuel*, 67, 666 (1988)
- 24) Hamilton R.T., Sams D.A., Shadman F., *Fuel*, 63, 1008 (1984)
- 25) Wood B.J., Sancier K.M., *Catalysis Review Science and Engineering*, 26, 233 (1984)
- 26) Gan H., Nandi S.P., Walke Jr P.L., *Fuel*, 51, 272 (1972)
- 27) Kannan M.P., Richards G.N., *Fuel*, 69, 747 (1990)
- 28) Zhu W., Song W., Lin W., *Fuel Process. Technol.*, 89, 890 (2008)
- 29) Suzuki T., Ohme H., Watanabe Y., *Energy Fuels*, 6, 343 (1992)
- 30) Cerfontain M.B., Moulijn J.A., *Fuel*, 65, 1349 (1986)
- 31) Takarada T., Ogiwara M., Kato K., *J. Chem. Eng. Jpn.*, 25, 44 (1992)